J Interv Card Electrophysiol (2017) 49:307–318
DOI 10.1007/s10840-017-0269-z

# Catheter ablation of atypical atrial flutter: a novel 3D anatomic mapping approach to quickly localize and terminate atypical atrial flutter

**Sri Sundaram[1] · William Choe[1] · J. Ryan Jordan[1] · Nate Mullins[2] · Charles Boorman[2] · Eric J. Kessler[3] · Sunil Nath[4]**

Received: 14 March 2017 / Accepted: 20 June 2017 / Published online: 29 June 2017


**Abstract**
*Purpose* This study aims to describe a novel method of High Density Activation Sequence Mapping combined with Voltage Gradient Mapping Overlay (HD-VGM) to quickly localize and terminate atypical atrial flutter.
*Methods* Twenty-one patients presenting with 26 different atypical atrial flutter circuits after a previous catheter or surgical AF ablation were studied. HD-VGM was performed with a commercially available impedance-based mapping system to locate and successfully ablate the critical isthmus of each tachycardia circuit. The results were compared to 21 consecutive historical control patients who had undergone an atypical flutter ablation without HD-VGM.
*Results* Twenty-six different atypical flutter circuits were evaluated. An average 3D anatomic mapping time of 12.39 ± 4.71 min was needed to collect 2996 ± 690 total points and 1016 ± 172 used mapping points. A mean of 195 ± 75 s of radiofrequency (RF) energy was needed to terminate the arrhythmias. The mean procedure time was 135 ± 46 min. With a mean follow-up 16 ± 9 months, 90% are in normal rhythm. In comparison to the control cohort, the study cohort had a shorter procedure time (135 ± 46 vs. 210 ± 41 min, $p = 0.0009$), fluoroscopy time (8.5 ± 3.7 vs. 17.7 ± 7.7 min, $p = 0.0021$), and success in termination of the arrhythmia during the procedure (100 vs. 68.2%, $p = 0.0230$).
*Conclusions* Ablation of atypical atrial flutter is challenging and time consuming. This case series shows that HD-VGM mapping can quickly localize and terminate an atypical flutter circuit.

**Keywords** Atypical atrial flutter · Ablation · 3D anatomic mapping · Atrial fibrillation · High density activation sequence mapping

**Abbreviations**

| | |
|---|---|
| AF | Atrial fibrillation |
| PAF | Paroxysmal atrial fibrillation |
| pAF | Persistent atrial fibrillation |

✉ Sri Sundaram
Sris@southdenver.com

William Choe
williamc@southdenver.com

J. Ryan Jordan
ryanj@southdenver.com

Nate Mullins
Nmullins02@sjm.com

Charles Boorman
cboorman@sjm.com

Eric J. Kessler
Ericjkessler@yahoo.com

Sunil Nath
rfablation@hotmail.com

[1] Cardiac Electrophysiology, South Denver Cardiology Associates, Littleton, CO 80120, USA

[2] St. Jude Medical, One St. Jude Medical Drive, St. Paul, MN 55117, USA

[3] Cardiac Electrophysiologist, Cardiac EP Consultants, 900 Technology Way, Libertyville, IL 60048, USA

[4] Colorado Springs Cardiology, 2222 N Nevada Ave, Suite 4007, Colorado Springs, CO 80907, USA

| | |
|---|---|
| HD-VGM | High Density Activation Sequence Mapping with Voltage Gradient Mapping Overlay |
| aAFL | Atypical atrial flutter |
| LA | Left atrium |
| RA | Right atrium |
| CS | Coronary Sinus |
| LAT | Local activation timing |
| RAI | Roving activation interval |
| LVID | Low-V ID |
| ACT | Activated clotting time |
| ICE | Intracardiac echo |
| LSI | Lesion size index |
| FTI | Force Time Integral |
| RF | Radiofrequency |
| CAFÉ | Complex atrial fractionated electrograms |

## 1 Introduction

Catheter ablation of drug refractory symptomatic atrial fibrillation (AF) has been shown to be an effective treatment [1–5]. While ablation of paroxysmal atrial fibrillation (PAF) has achieved a high rate of success with one procedure, ablation of persistent atrial fibrillation (pAF) with a single procedure has not been as successful. Recurrences in pAF patients can manifest as atypical atrial flutters (aAFL) which are difficult to treat medically [6–8]. This can occur if linear ablation lesion sets are delivered, during the index procedure [9–12]. Ablation of aAFL can be challenging with limited success and long procedural times [13–15]. In this multicenter, retrospective case series, we report a novel method with High Density Activation Sequence Mapping combined with Voltage Gradient Mapping Overlay (HD-VGM) with an impedance-based electroanatomic mapping system (EnSite Velocity, St. Jude Medical, St. Paul, MN, USA) to identify the highest voltage areas within the slowest zones of conduction. This method shows the critical zones of conduction that can be targeted for successful ablation.

## 2 Methods

### 2.1 Study population

The study population consisted of 21consecutive patients (17 male and 4 female), presenting with 26 separate symptomatic, drug refractory, aAFL. All had a prior history of AF and had undergone at least one prior catheter or surgical ablation procedure for AF. The procedures were performed at three separate institutions by four different operators. Patients were only included if they had a stable tachycardia cycle length. The baseline characteristics of the study patients are described in Table 1.

The study population was compared to a historical cohort of 21 patients who had undergone an aAFL ablation prior to the use of HD-VGM and release of contact force catheters. The comparison cohort had undergone ablation with standard mapping methods and pacing maneuvers such as entrainment mapping. The control cohort had their procedures performed at the same three institutions by the same four operators as the study cohort. Baseline characteristics of the control cohort are described in Table 1; the procedure data is described in Table 2.

This study was approved by our local institutional review board.

### 2.2 Previous ablation procedures

All patients had at least one prior pulmonary vein isolation procedure (PVI) with either catheter-based or surgical ablation. Catheter-based procedures were performed with an ablation catheter of the operator's choice. Additionally, the operator performed, a mitral isthmus line, roof line and/or complex fractionated atrial electrogram (CAFÉ) ablation lesion sets at their discretion. Ablation lesions were limited to the left atrium (LA) for prior catheter-based procedures. The post-surgical patients had both left and right atrial ablations with a combination of RF and cryoablation.

### 2.3 Statistical analysis

All values are reported as mean ± standard deviation. Study and control groups were compared using parametric (Student's *t* test) and nonparametric (Wilcoxon rank sum test) tests for continuous variables as appropriate and Fisher's exact test for categorical data (SAS Version 9.4, Cary, NC). A $p$ value $<0.05$ was considered statistically significant.

### 2.4 Mapping and data collection

The 3D mapping system was set up with a coronary sinus (CS) electrogram as the mapping reference. The usual setup has been described previously [16]. The CS reference electrogram was selected based on the amplitude and consistency [17].

A multi-electrode spiral catheter (Reflection Spiral, St. Jude Medical, St. Paul, MN USA) with equally spaced electrodes (6.3 mm) was selected as the roving catheter (ROV) and configured to collect local activation timing (LAT) from all bipolar (or paired bipolar if interelectrode spacing was unequal) signals simultaneously. The signal detection of absolute peak (Abs peak) was used on the ROV. Abs peak is defined as the largest amplitude, either positive or negative, of the bipolar signal and coincides with the -dv/dt on a unipolar signal. The near-field signal has long been defined in a unipole as the –dv/dt. This simply means that the near-field signal in a bipole is commonly defined as the Abs peak. In fact, the Abs

**Table 1** Patient characteristics

| Data | Results Study cohort | Results Control cohort | *p* value |
|---|---|---|---|
| Age | 63 ± 5 | 62 ± 10 | 0.65 |
| Male | 17 (81%) | 15 (71%) | 0.32 |
| LVEF | 50% (±5) | 56% (±10) | 0.10 |
| LA size | 4.54 cm (±0.53) | 4.46 cm (±0.69) | 0.77 |
| $CHA_2DS_2$-VASC score | 1.4 (±1.7) | 1.9 (±1.3) | 0.25 |
| DM | 3 (14%) | 5 (23%) | |
| HTN | 3 (14%) | 5 (23%) | |
| CAD | 2 (10%) | 2 (10%) | |
| CHF | 1 (5%) | 2 (9%) | |
| Prior ablation | | | |
| PVI only | 5 | 7 | |
| PVI + additional sites | 11 | 12 | |
| Surgical MAZE | 5 | 2 | |
| Mean days since index procedure | 1254 (±1323) | 1003 (±417) | 0.11 |

**Table 2** Procedure data for study subjects

| Patient | # of circuits | Index procedure | LA size (CM) | Location of circuit | Cycle length of flutter circuit | Total points taken | Total points used | Mapping time (min) | Ablation time (s) | Total procedure time (min) |
|---|---|---|---|---|---|---|---|---|---|---|
| 1 | 1 | PVI, CAFE | 4.1 | MI | 247 | 1317 | 699 | 8:25 | 90 | 74 |
| 2 | 1 | MAZE | 4.4 | LA roof | 250 | 3368 | 775 | 10:00 | 30 | 63 |
| 3 | 2 | PVI, CAFÉ, ROOF | 3.5 | LA roof | 220, 280 | 1387, 1704 | 758, 847 | 10:00, 9:00 | 240, 150 | 193 |
| 4 | 1 | CAFÉ, ROOF | 4.5 | RA | 370 | 813 | 306 | 13:50 | 30 | 120 |
| 5 | 1 | MAZE | 4.5 | MI | 300 | 1398 | 630 | 13:00 | 30 | 120 |
| 6 | 1 | PVI ROOF | 4.5 | MI | 225 | 1453 | 592 | 7:12 | 120 | 180 |
| 7 | 1 | PVI, ROOF | 3.6 | MI | 340 | 1472 | 622 | 21:00 | 30 | 170 |
| 8 | 4 | PVI, CAFÉ, ROOF | 4.5 | MI, LA roof, CTI, focal | 220,210 200, 206 | 1172, 696, 880, 691 | 612,400, 500,296 | 13:00, 10:00,9:00 8:00 | 90, 90, 180, 240 | 360 |
| 9 | 1 | PVI | 3.1 | Focal | 240 | 1033 | 633 | 8:00 | 90 | 132 |
| 10 | 1 | PVI, ROOF | 4.2 | Focal | 245 | 1733 | 656 | 10:00 | 240 | 115 |
| 11 | 1 | PVI, ROOF | 4.5 | MI | 209 | 3619 | 1314 | 12:00 | 90 | 125 |
| 12 | 1 | PVI | 5.4 | MI | 215 | 1795 | 821 | 6:30 | 120 | 66 |
| 13 | 1 | MAZE | 4.5 | RA | 220 | 2463 | 1314 | 18:52 | 180 | 90 |
| 14 | 1 | PVI, ROOF, CAFE | 6.7 | LA roof | 270 | 8844 | 2162 | 11:00 | 120 | 111 |
| 15 | 1 | PVI, ROOF | 4.8 | Focal | 400 | 8474 | 1278 | 15:00 | 120 | 120 |
| 16 | 1 | PVI, CAFE | 4.5 | Roof | 260 | 1392 | 675 | 9:53 | 200 | 60 |
| 17 | 1 | PVI | 5.7 | Roof | 400 | 2215 | 1454 | 21:00 | 120 | 249 |
| 18 | 1 | MAZE | 5.9 | LA antrum | 310 | 8843 | 2684 | 20:00 | 571 | 259 |
| 19 | 2 | MAZE | 5.9 | LA posterior wall | 220/230 | 7508 2228 | 1705 458 | 15:00 6:00 | 526 526 | 159 |
| 20 | 1 | PVI | 3.6 | Roof | 220 | 9324 | 3353 | 18:00 | 407 | 200 |
| 21 | 1 | PVI | 4.4 | Roof | 240 | 2083 | 878 | 23:00 | 180 | 94 |

*PVI* pulmonary vein isolation, *CAFÉ* complex atrial fractionated electrogram mapping, *ROOF* roof line in LA connecting the PVI lines from RUPV to LUPV, *MAZE* combination of right and left atrial ablation with Cryo and RF energy, *LA* left atrium, *RA* right atrium, *CTI* cavotricuspid isthmus

peak appropriately identifies the near-field deflection even when multiple potentials are seen. The sensitivity was adjusted for the ROV to a maximum value of 10 mV to ensure the largest amplitude bipolar signal was selected, rather than the first signal in our roving activation interval (RAI). The RAI window was setup to include 95% of the cycle length of the tachycardia. For all patients, the entire cycle length was captured in the chamber of interest. Intracardiac signals were assessed for noise and a 60-Hz notch/noise filter was applied if 60 Hz noise was present. Interior and exterior projection values were set at 5 mm, rather than the default values of 15 mm. This keeps any intracavitary data from being used in the map. The interpolation value was also set to 5 mm, rather than the default value of 10 mm. With this setting, regions of the 3D map containing missing LAT data was easily visible to the operator and targeted for further data collection.

After the data was collected with the multi-electrode spiral catheter, two methods of data interpretation were performed:

First, the EnSite mapping system was set to display all mapping points with only eight isochronal color bands in the following activation pattern: white ➔red ➔ orange➔ yellow ➔ green ➔ light blue ➔ dark blue ➔ purple. Interpretation of the map is simplified with this limited color palate. Each color band represents equally spaced timing. Therefore, large and wide color bands represent fast conduction, while tightly spaced color bands represent slow conduction. The color sequence must follow this order. For instance, if there is an area of non-sequential coloring, this indicates that the electrical

**Table 3** Procedure data for control subjects

| Patient | # of circuits | Index procedure | LA size (CM) | Location of circuit | Total procedure time (min) | Successful ablation |
|---|---|---|---|---|---|---|
| 1 | 1 | PVI, ROOF, CAFE | 4.7 | MI | 180 | No (bidirectional block was not achieved) |
| 2 | 2 | PVI | 4.0 | Roof | 270 | No (bidirectional block was not achieved on roof, tachycardia was reinducible) |
| 3 | 1 | PVI, ROOF, MI CAFÉ | 4.0 | Focal—anterior wall | 270 | Yes |
| 4 | | PVI | 3.2 | Roof, anterior wall | 180 | Yes |
| 5 | | PVI, ROOF | 6.0 | Appendage, anterior wall | 150 | No (tachycardia could not be terminated) |
| 6 | | PVI | 3.4 | Focal | 150 | Yes |
| 7 | | PVI | 4.7 | Focal | 210 | Yes |
| 8 | | PVI | 4.8<br>4.2 | MI, roof | 180 | Yes |
| 9 | | PVI, ROOF | 4.1 | Anterior wall | 210 | Yes |
| 10 | | PVI | 4.7 | MI | 240 | Yes |
| 11 | | PVI, ROOF, MI, CAFE | 4.6 | MI | 150 | Yes |
| 12 | | PVI, ROOF, CAFÉ | 4.1 | Posterior wall | 210 | Yes |
| 13 | | PVI, ROOF | 4.8 | Roof | 300 | No (bidirectional block not achieved on roof. Patient also had recurrent MI flutter) |
| 14 | | PVI, ROOF | 5.6 | MI, CTI | 240 | Yes |
| 15 | | PVI | 3.6 | Roof | 180 | Yes |
| 16 | | PVI | 5.3 | Multiple LA anterior wall circuits | 180 | No (unable to localize circuit) |
| 17 | | PVI, ROOF | 4.8 | Appendage | 180 | Yes |
| 18 | | PVI | 5.6 | Multiple LA anterior wall circuits | 240 | No (unable to localize circuit) |
| 19 | | PVI | 3.6 | Roof | 240 | Yes |
| 20 | | PVI, ROOF, MI | 5.3 | LA posterior wall, CTI, roof | 240 | No (unable to localize posterior wall circuit) |
| 21 | | MAZE | 4.8 | Posterior wall | 180 | Yes |

*PVI* pulmonary vein isolation, *CAFÉ* complex atrial fractionated electrogram mapping, *ROOF* roof line in LA connecting the PVI lines from RUPV to LUPV, *MAZE* combination of right and left atrial ablation with Cryo and RF energy, *LA* left atrium, *RA* right atrium, *CTI* cavotricuspid isthmus

activation, in that region, takes another route through the tissue to get to that location. With only eight colors to analyze, following the sequence of activation is simplified.

The second method of data interpretation that was performed was with the LVID setting in the Mapping Control Panel. Using the same data that was collected in method one, voltage values were annotated automatically on the EnSite system and stored for each LAT point. The Low-V ID (LVID) was selected with the nominal setting of 1.0 mV. With this setting, an area of voltage lower than 1.0 mV will display as gray on the 3D map, which signifies scar. In brief, the LVID identifies low-voltage zones in activation maps. If a collected LAT point has a peak-to-peak (P-P) value lower than the specified LVID value, that point will display as gray and not be included in the color-coded timing scale. This helps to eliminate LAT points collected that were baseline noise on the electrogram. By increasing the LVID to a higher voltage value, more of the mapping data appears as gray or "scar." Similarly, by decreasing the LVID, more of the mapping data appears as active tissue and is used in the activation mapping. The LVID is dynamically adjusted until only the largest voltage area in the previously identified critical slow conduction zone is shown. A narrow channel of higher voltage then becomes apparent in the slow conduction zone. After the target area was identified with HD-GVM, additional data points were obtained, in this identified area, with a 3.5-mm irrigated tip contact sensing ablation catheter (Tacticath catheter (St. Jude Medical, St. Paul, MN)). Points were only taken when contact force was greater than 10 g and less than 40 g. Collecting additional data points with the contact sensing catheter further defined the area targeted for ablation.

### 2.5 Patient management

Patients were brought into the cardiac electrophysiology laboratory (EP Lab) in a fasting state. All patients were in spontaneous aAFL at the time of the procedure. Antiarrhythmic medications were discontinued at least 48 h prior to the procedure. Amiodarone was discontinued 1 month prior to the procedure. Anticoagulant discontinuation was at the discretion of the operator. Patients underwent a pre-procedural CT scan and transesophageal echo if clinically indicated. All procedures were performed under general anesthesia. Intracardiac echo (ICE) was utilized for transseptal access and imaging in all LA procedures. Heparin was bolused to achieve an activated clotting time (ACT) of 300 s or greater prior to accessing

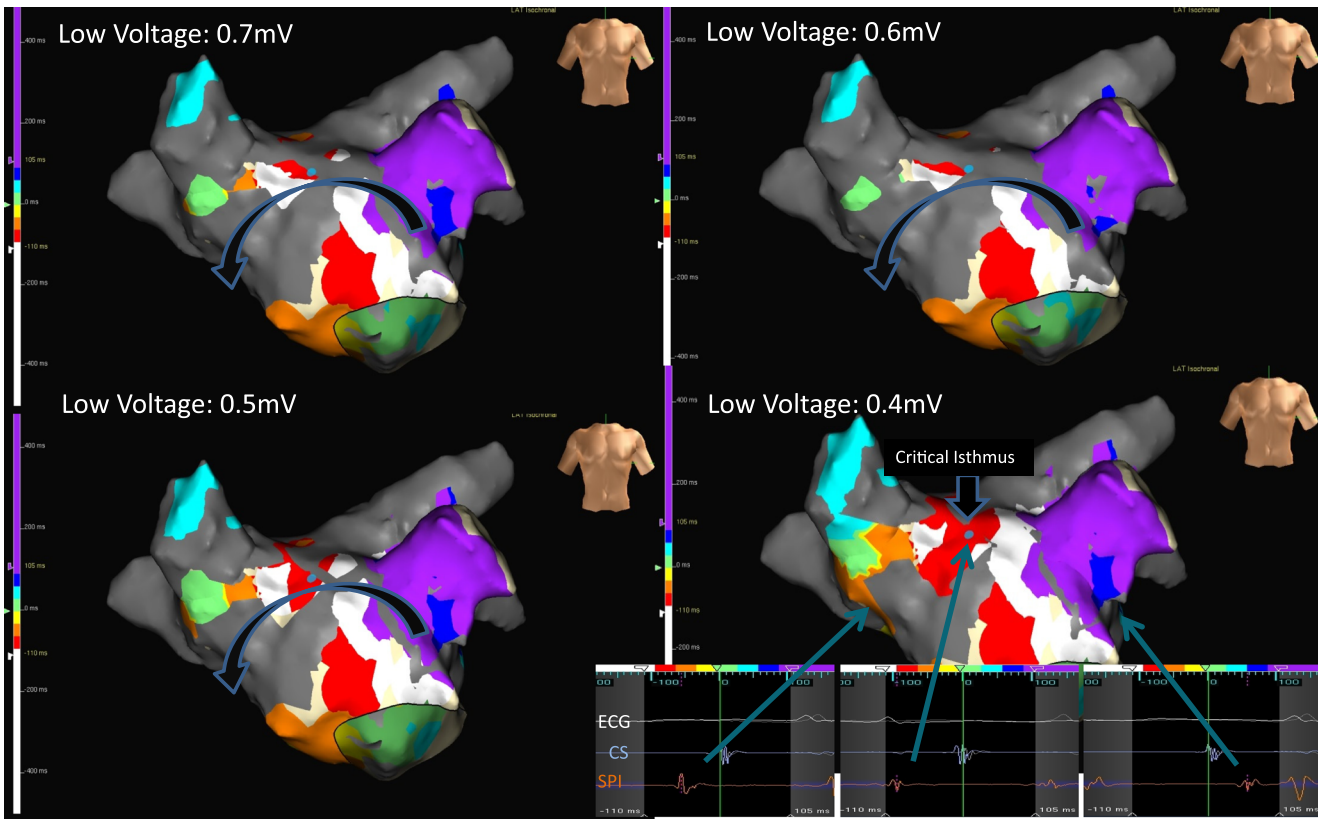


**Fig 1** Anterior projection of the left atrium showing a left atrial flutter traveling counterclockwise around the mitral valve. There are different levels of low-voltage overlay values (Low-V ID) on each panel. The value was dynamically adjusted until a channel or critical isthmus appears at 0.400 mV. The termination was annotated by the *blue dot* on the *lower right panel*. *CS* coronary sinus, *SPL* spiral catheter

the LA. A continuous infusion of heparin was employed to maintain an ACT greater than 300 s during the case. A decapolar CS catheter (Livewire, St. Jude Medical, St. Paul, MN, USA) was advanced and used as a reference during the case. Its location was shadowed to maintain a stable reference throughout. In LA cases, a fixed sheath (SL-1, St. Jude Medical, St. Paul, MN, USA) and a steerable transseptal sheath (Agilis, St. Jude Medical, St. Paul, MN, USA) were advanced into the LA. For RA cases, the ablation catheter was advanced without the aid of a sheath or with the use of an SR-0 sheath.

Using Ensite, geometries of the LA, RA, and pulmonary veins were acquired using a decapolar circular mapping catheter (Reflexion Spiral, St. Jude Medical, St. Paul, MN USA). This map was compared with the anatomy from the CT scan acquired prior to the ablation for a reference. In all patients with prior catheter or surgical ablation of the LA, the pulmonary veins were first evaluated. If electrical activity was noted in the veins, these areas were re-isolated with RF ablation. The aAFL was then evaluated with HD mapping as described above. Traditional methods to determine the site of activation such as entrainment mapping was not utilized.

Once areas of ablation were targeted, the Tacticath 3.5 mm catheter was placed through a long sheath and advanced into the targeted chamber. Ablation lesions were delivered with the Ampere RF ablation generator (St. Jude Medical Inc., St. Paul, MN, USA) to achieve energy up to 25–35 W at 40 C for a maximum of 60 s in each location. Lesions in the posterior LA were limited to 25 W. All patients were in a spontaneous aAFL at the time of the procedure. If the tachycardia terminated, re-induction was performed with rapid atrial pacing down to 200 ms with and without isoproterenol from 5 to 20 μg/ml. If tachycardia was not induced, the ablation was considered successful. If a new tachycardia was induced, it was similarly targeted for mapping and ablation. A separate map was made for each arrhythmia that was induced. Linear ablation to form a complete line with block was not attempted. At the completion of the case, all patients were in sinus rhythm. All patients were observed overnight and discharged the next day. All patients had outpatient evaluations at 1 and 2 weeks post ablation. In addition, patients were seen at 3, 6, and 12 months post ablation. Additional follow-up was directed by clinical indications. For recurrences of PAF or aAFL, the arrhythmia was documented with an ECG and then a cardioversion was performed within 48–72 h for persistent episodes within the first 3-month blanking period. After the 3-month blanking period was completed, all patients had a 2 week continuous monitor. In accordance with the Heart

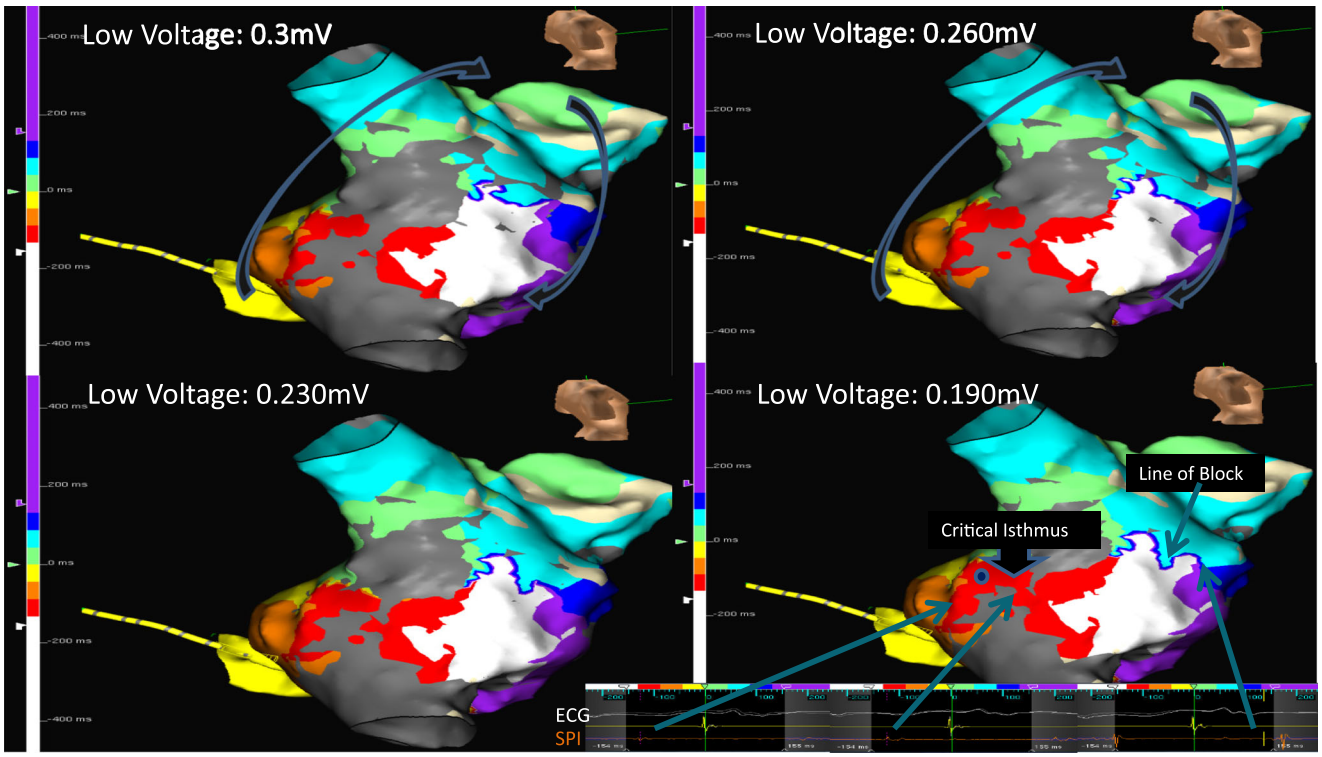


**Fig 2** Right lateral projection of the right atrium showing a right atrial scar mediated flutter. The varying levels of Low-V ID are depicted on each panel. The value was dynamically adjusted until a channel or critical isthmus appeared at 0.190 mV. Note the line of block in the chamber in the *lower right image*. The *light blue timing area* is directly next to the *white timing area*. This doesn't follow the color scheme and therefore represents an area of conduction block. At the critical isthmus (*in the red area*), there was phrenic nerve stimulation. Ablation with termination was annotated by the *blue dot* in the *lower right panel*

Rhythm Society guidelines, all patients were followed for 1 year with ECGs for documentation of any symptomatic episodes [18]. Anticoagulation was continued at least 3 months and then guided by the individual patient's $CHA_2DS_2$-VASc score.

## 3 Results

A total of 26 different circuits were evaluated in 21 different patients. With this novel method of HD-VGM, the average time for collecting the mapping points and analysis was 12.39 (±4.71) min. An average of 2996 (+690) points of interest were collected and 1016 (±172) points were used to create and analyze the map. A critical isthmus was identified in all 26 circuits. Once this analysis was performed, the arrhythmias were targeted and successfully treated with 195 (±75) s of RF ablation energy. For two patients, the RF ablation time was significantly longer than the mean time as the critical isthmus was larger and adequate contact was difficult to obtain with the ablation catheter. The mean total procedure time was 135 (±46) min. All 26 of the flutter circuits were successfully terminated during the ablation. With a mean follow-up of 16 (±9) months (12/21 patients were greater than 1 year), 19/21 (90%) patients have remained in normal rhythm off antiarrhythmic medication. Of the two recurrences, one patient had a recurrence of an atrial tachycardia from the left atrial appendage, which was a different arrhythmia than the prior procedure. This was successfully ablated on a subsequent procedure. The other patient declined ablation and chose antiarrhythmic drug therapy. HD-VGM was used successfully to treat multiple flutters in both the RA and LA. Additionally, patients that have undergone both catheter and surgical ablation were successfully treated. There were no complications noted in this cohort Table 3.

In comparison to the control group that had previously undergone an aAFL ablation with traditional methods, the study cohort had a shorter procedure time (135 ± 46 vs. 210 ± 41 min, $p = 0.0009$), fluoroscopy time (8.5 ± 3.7 vs. 17.7 ± 7.7 min, $p = 0.0021$), and overall success in termination of the atypical atrial flutter during ablation (100 vs. 68.2%, $p = 0.0230$).

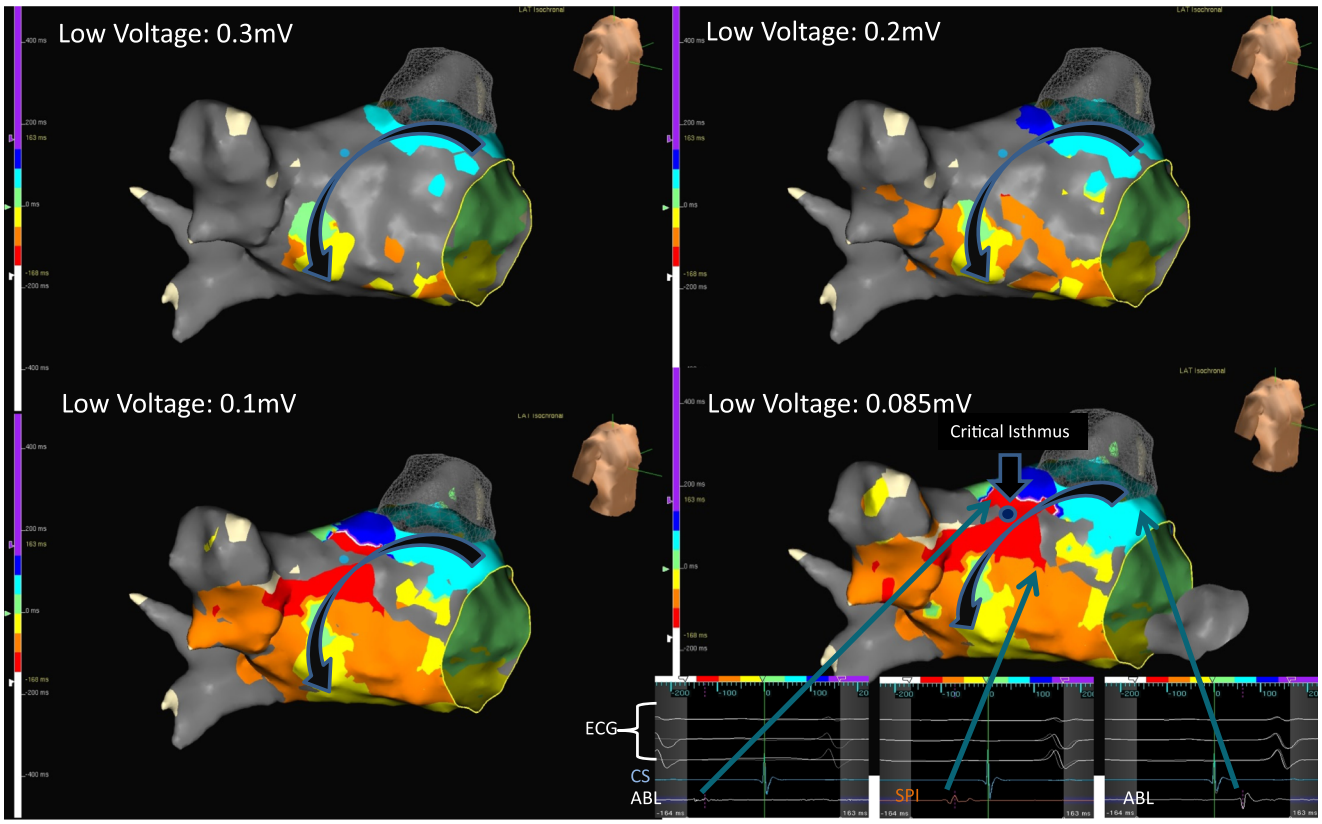


**Fig 3** Right lateral projection of a left atrial flutter traveling counterclockwise around the mitral valve. Low-V ID thresholds cause any signals below that value to appear gray. This value was dynamically adjusted until a channel or critical isthmus appeared at 0.085 mV. The critical isthmus is identified in the *lower right panel*. The termination was annotated by the *blue dot* on the *lower right panel* in the critical isthmus. *ABL* ablation catheter

## 4 Discussion

The HD-VGM method of mapping and interpretation is different than the currently accepted methods because it utilizes a voltage map overlaid on a local activation timing map. By combining both maps, the highest voltage within the critical slow zones of conduction can be rapidly identified and targeted for ablation. Using the Ensite 3D mapping system to create a high-density map of cardiac chambers has been demonstrated previously [19–21]. The combination of the voltage map overlaid on the activation map that has only recently been evaluated [22]. The comparison of the HD-VGM method to traditional mapping methods with procedure results, however, has not been previously described (see Figs. 1, 2, 3, 4, 5, 6, and 7).

Identification of the location of the circuit was accomplished exclusively with a 3D mapping system that is currently widely available. No additional system upgrades are required to perform the HD-VGM. This novel method of HD-VGM acquired with a multipolar catheter also differs from more traditional methods of mapping because rapid collection of data points is collected without a significant amount of editing by the operator. The 3D anatomic mapping system is capable of annotating each point appropriately without the operator editing the location of the timing caliper. This is done primarily by choosing the Abs peak of the bipolar electrogram on the ROV, rather than the onset or –dv/dt. The onset of bipolar electrogram activation and maximum –dv/dt alone sometimes do not represent near-field activation due to limitations in both methods. By using the EnSite system's ability to detect a peak electrogram, there can be automated collection of data. If the –dv/dt or onset was used; this would require beat-by-beat manual analysis by the operator. These improvements in the data collection allow for a more rapid construction of a 3D anatomic map. Compared to prior studies evaluating aAFLs, the total procedure time is significantly reduced [23]. In addition, compared to the prior 21 consecutive, historical patients that had aAFL ablation, there was a 75-min reduction in procedure time.

Another difference between HD-VGM and more traditional methods is the identification of the circuit of interest. Based on the simplified color scheme, the operator can easily determine the difference between active tissue channel within the circuit and passively activated tissue channels. The main method to determine if the circuit is active or passive is to identify all of the colors in the spectrum as a connected series.

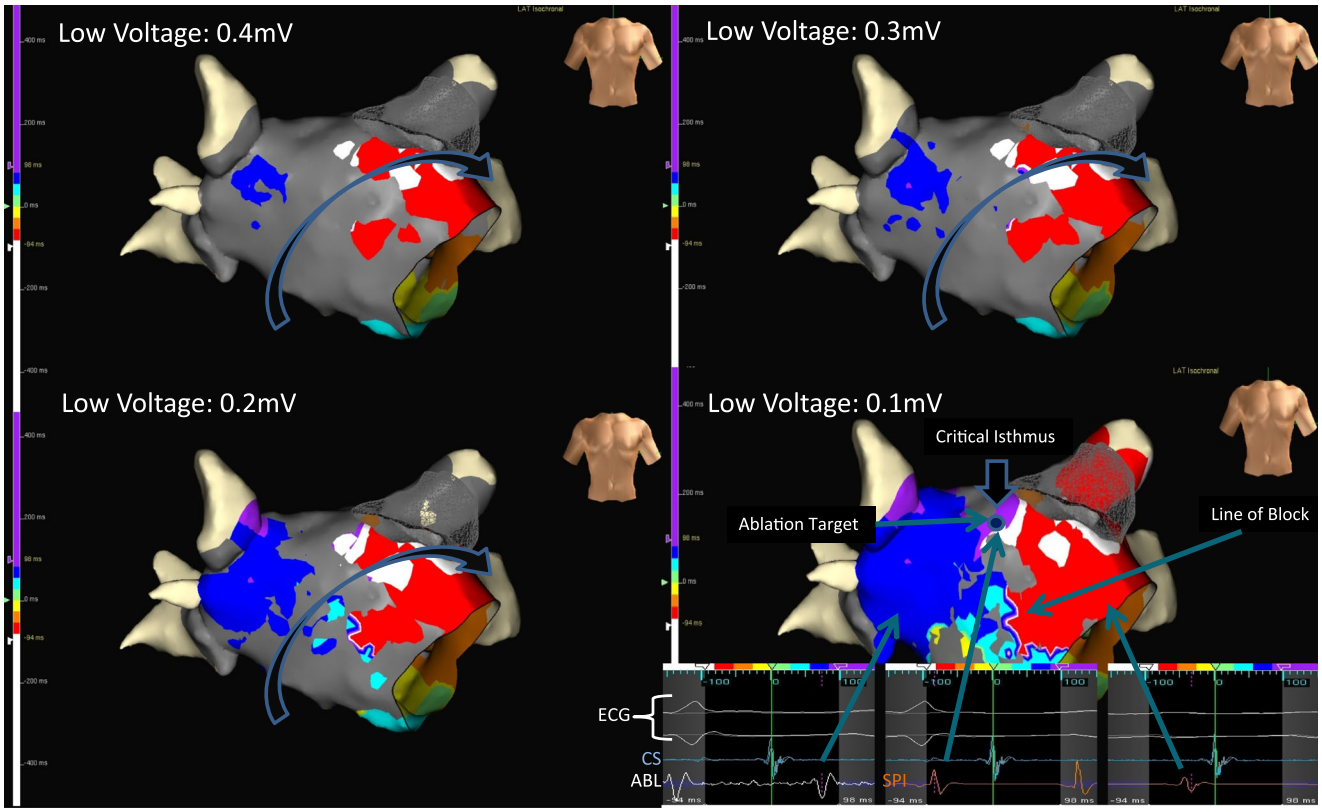


**Fig 4** Anterior projection of a left atrial flutter traveling clockwise around the mitral valve. Low-V ID thresholds cause any signals below the set value to appear as gray. This value is dynamically adjusted until a critical isthmus appeared at 0.1 mV. The critical isthmus is identified in the *lower right panel*. This is clearly seen as the *red* is near the *light blue*. This doesn't follow the color scheme and, therefore, represents an area of conduction block. From a previous ablation, there is a line of block on the anterior surface near the mitral. With ablation in the critical isthmus (*white and purple narrow bands*), the tachycardia terminated

If the circuit is active, all of the colors in the activation sequence flow in order and the early and late areas meet. The critical circuit will have the pattern of White ➔Red ➔ Orange➔ Yellow ➔ Green ➔ Light blue ➔ Dark blue ➔ Purple.

If an area of tissue is identified and does not have all of the colors in the spectrum, or if the colors are out of sequence, this must be via passively activating tissue or with two passive wave fronts colliding. These areas are, subsequently, not targeted for ablation. For instance, in Fig. 5c, area 1 is a passive area of conduction. The activation sequence does not follow the color sequence. Instead, the color sequence is White ➔ Red ➔ Orange ➔Yellow ➔ Green ➔ Purple. The transition from Green ➔ Purple does not follow the designated activation pattern. Therefore, the border between Green ➔ Purple must be a line of functional block. Activation of the Purple area must be from adjacent areas in the anterior of the LA. Similarly, in Fig. 5c, area 3, the activation is from White ➔ Red ➔ Orange ➔ Dark Blue. The transition from Orange➔ Dark Blue does not follow the designated activation pattern. Therefore, the border between Orange and Dark Blue must be line of functional block and the Dark Blue area is activated from adjacent areas in the anterior wall. These areas do not represent an area of focus for therapy.

The combination of the color scheme with the voltage map is a unique method. In Fig. 5b, there are three possible voltage bridges noted and labeled as areas 1, 2, and 3. If voltage was the only criteria used, all three could be targeted for ablation. As shown in panel c, ablation of area 2 only would lead to termination of the arrhythmia. Areas 1 and 3 would not

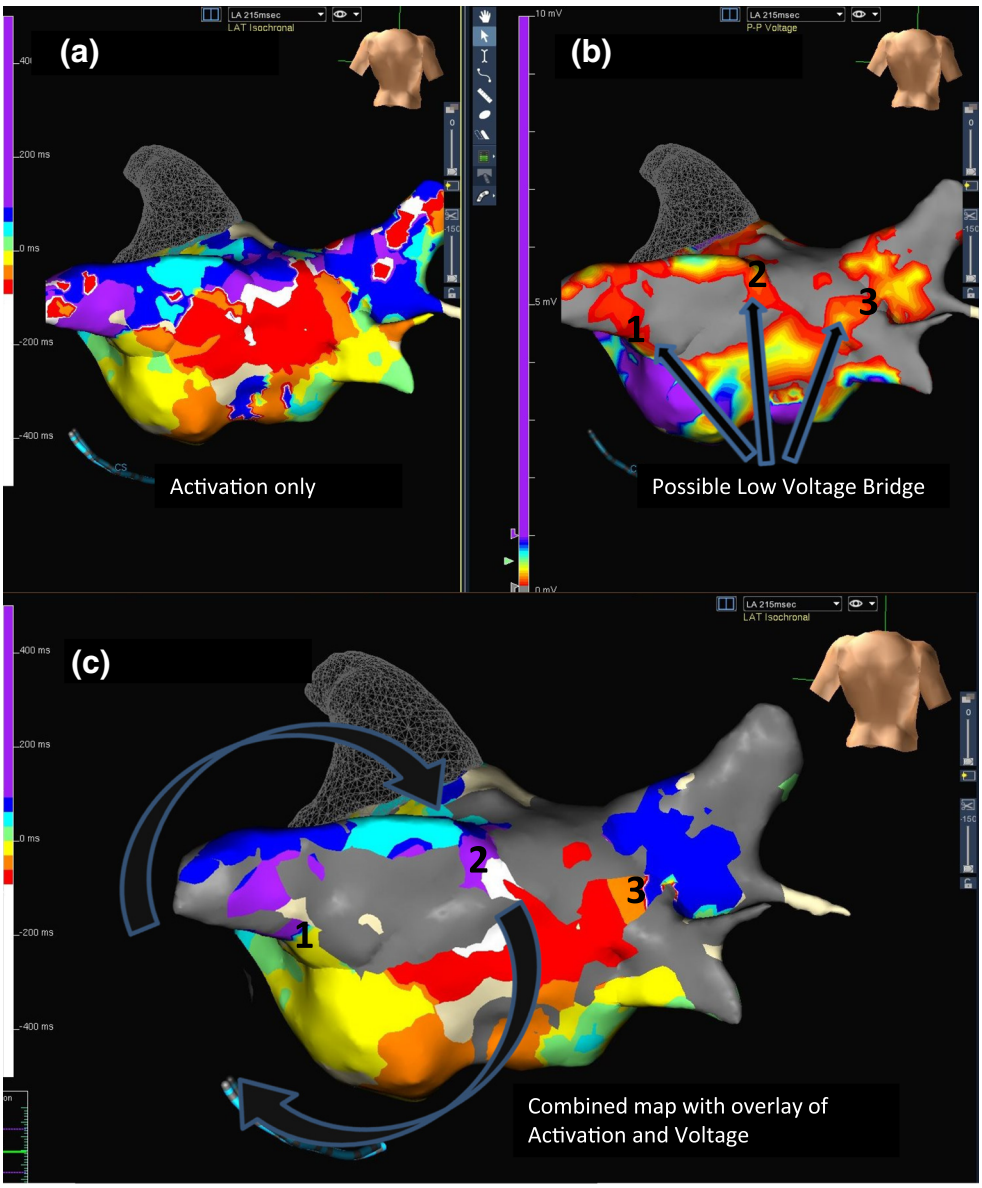


**Fig. 5** Posterior view of LA of an atypical atrial flutter. **a** An activation only map that shows the tachycardia circuit traversing the roof. Using the data from **a** only, a roof line would be targeted, as this has the most color compression, indicating a slow zone. The tachycardia would terminate but with ablation of a larger area than is required. **b** A voltage map only. Using the data from this panel, three different voltage bridges could be targeted for ablation. Voltage bridges 1 and 3 would not terminate the tachycardia. **c** The overlay of activation and voltage. By combining both maps, the highest voltage area within the slow zone becomes apparent. Voltage bridge 2 has all the colors in sequence and can be targeted with minimal ablation. Panel **c** also shows why voltage bridge 1 and 3 would not terminate the tachycardia. These are high-voltage areas but the activation pattern does not follow color sequence

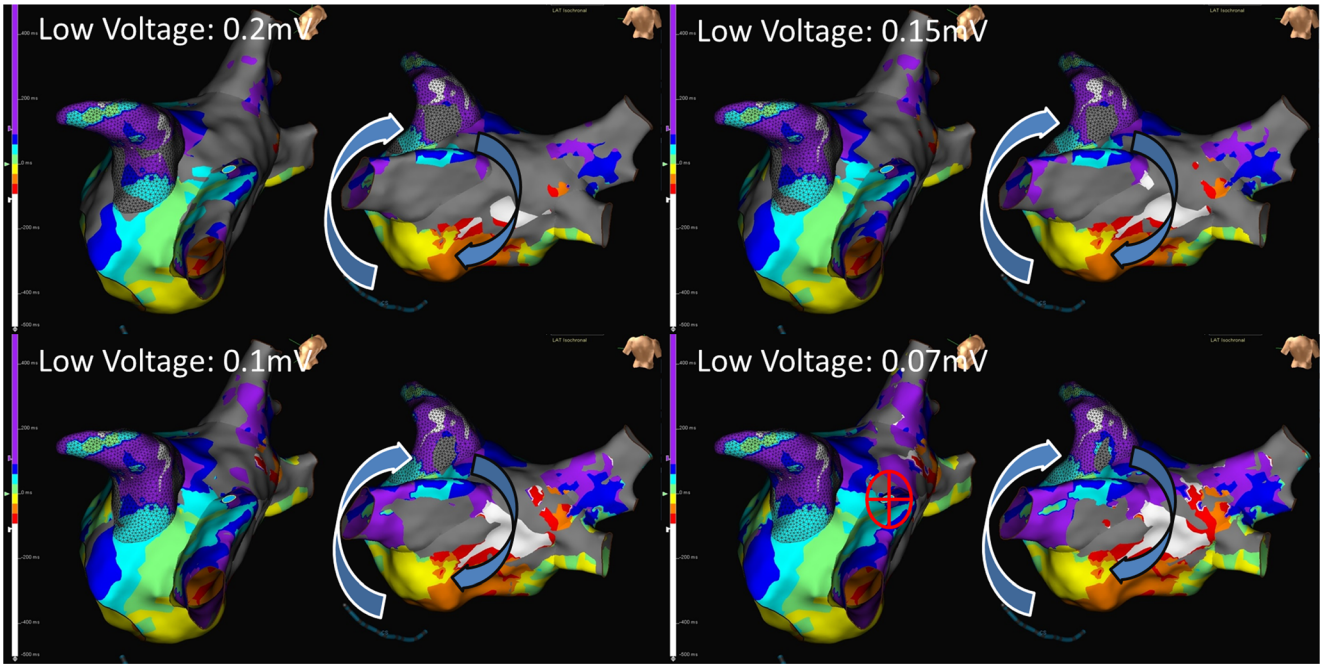


**Fig. 6** The tachycardia was noted to travel around the left lower pulmonary vein to the mitral isthmus region. The mitral isthmus region had the most color compression and, therefore, was the slowest part of the circuit. The shortest area of ablation, however, was the top of the left common vein between the vein and left atrial appendage. This area was targeted and successfully ablated

terminate the tachycardia as they are not part of the critical circuit. These areas do not have the necessary color sequence for successful ablation. For this reason, voltage mapping alone may not correctly identify the area of termination. Figure 5a is an activation map only. With this map, the entire LA roof could be targeted and would successfully terminate the

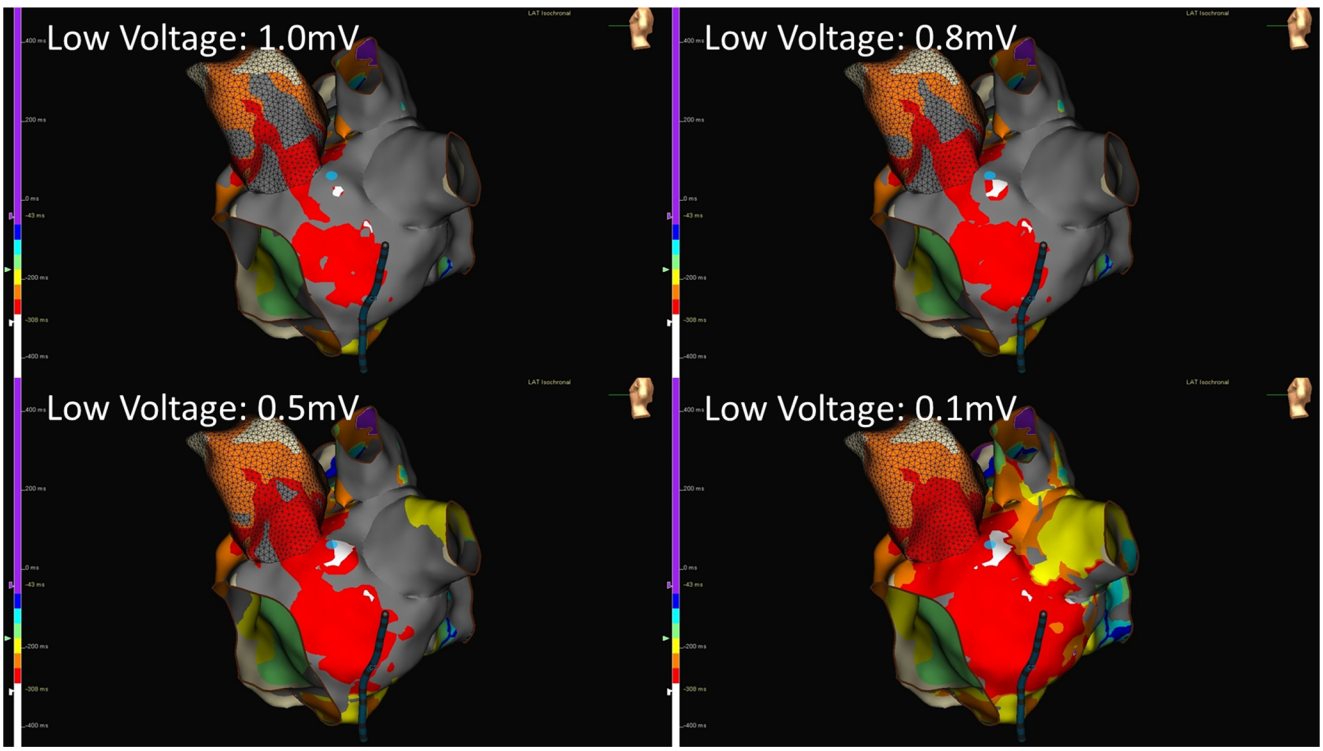


**Fig. 7** A critical focal source appears in the 0.1 mV image. There is a focal area of white tissue located between the LA appendage and the left lower pulmonary vein. The focal white area is the earliest activation time and is *surrounded by red* and then the remainder of the color sequence. This *white area* was successfully targeted for ablation

tachycardia but with more ablation lesions than are necessary. By combining both the activation map with the color sequence, as shown in panel c, the critical part of the circuit is easily identified and targeted for ablation. Once the active circuit is identified, voltage gradient mapping can be done to show the specific focus of the highest voltage areas within the slow conducting zones of the tachycardia.

Winkle et al. recently described a technique similar to HD-VGM, using high-density mapping with a combination of voltage and activation to map the entire flutter circuit [22]. Our study expands upon this concept, showing that the successful site of ablation is the high-voltage area within the slow zone of conduction. By focusing on the critical high-voltage area, within the slow zone, we were able to terminate the arrhythmia with minimal ablation lesions. If the entire high-voltage area is not ablated, the arrhythmia may reoccur. Our focus on this critical area within the slow zone is the likely the reason that our 1 year success rate was higher (90%) than in Winkle et al.'s prior study (61%). Additionally, we show for the first time improved procedural outcomes using high-density mapping as compared to traditional mapping. In this study, we show that total procedure time, fluoroscopy time, and RF application time were decreased compared to more traditional methods. This manuscript is also unique in that it describes the specific alterations to the Ensite system that are necessary for an electrophysiologist to perform high-density activation mapping. Increased utilization of the EnSite velocity system in this publication eliminate the need for manual edits of the data, leading to quicker identification of the circuit (12 vs. 20 min).

## 5 Limitations

The main limitation of this study is the small sample size of cases reviewed. Further studies with larger number of patients followed for a longer time period are necessary to confirm the feasibility of this technique.

Additionally, the 3D map's accuracy is contingent upon accurate contact voltage data. Most of the points not in contact can be excluded with interior projection value along with a proper LVID setting. It is essential to exclude premature beats, ventricular measurements, and catheter artifact. In addition, the data points were not analyzed manually by the operator. This was done to increase the speed of data collection and analysis. The trade-off for the increased speed is that errors in notation could have been made and accounted for in the 3D maps. While this is a more efficient way of collecting data, it is not automated such as other systems currently available. Also, as traditional methods to locate the flutter circuit, such as entrainment mapping, was not performed, validation of this method with currently accepted methods cannot be made. Another limitation is that the data from the historical cohort of 21 patients was obtained prior to the release of contact sensing catheters.

## 6 Conclusion

Ablation of aAFLs is a challenging and frequently time-consuming procedure. This case series shows that this HD-VGM technique, which is currently commercially available, can be used to efficiently map and ablate these rhythms. Multiple operators at three different institutions were able to successfully ablate aAFL rapidly using this technique. With this method, procedure and fluoroscopy times can be reduced and acute success rates increased.

**Acknowledgments** The authors thank Ms. Kim Oaks for the editorial assistance and Ms. Manya Harsch for the statistical assistance.

**Compliance with ethical standards** This study was approved by our local institutional review board.

**Conflict of interest** Drs. Sundaram and Choe are on the speaker's bureau for St. Jude Medical. In addition, Drs. Sundaram and Choe have received a research grant from St. Jude Medical, Asia Division, to study the genetic basis of Brugada Syndrome in Cambodia. This conflict is not relevant to the article. N. Mullins and C. Boorman receive salary support from St. Jude Medical.

## References

1. Haissaguerre M, Jais P, Shah DC, Takahashi A, Hocini M, Quiniou G, et al. Spontaneous initiation of atrial fibrillation by ectopic beats originating in the pulmonary veins. NEJM. 1998;339:659–66.
2. Haissaguerre M, Shah DC, Jais P, Hocini M, Yamane T, Deisenhofer I, et al. Electrophysiological breakthroughs from the left atrium to the pulmonary veins. Circulation. 2000;102:2463–5.
3. Haissaguerre M, Jais P, Shah DC, Garrigue S, Takahashi A, Lavergne T, et al. Electrophysiological end point for catheter ablation of atrial fibrillation initiated from multiple pulmonary venous foci. Circulation. 2000;101:1409–17.
4. Papone C, Rosanio S, Oreto G, Tocchi M, Gugliotta F, et al. Circumferential radiofrequency ablation of pulmonary vein ostia: a new anatomic approach for curing atrial fibrillation. Circulation. 2000;102:2619–28.
5. Oral H, Scharf C, Chugh A, Hall B, Cheung P, et al. Catheter ablation for paroxysmal atrial fibrillation: segmental pulmonary vein ostial ablation versus left atrial ablation. Circulation. 2003;108:2355–60.
6. Haissaguerre M, Hocini M, Sanders P, Sacher P, Sacher F, et al. Catheter ablation of long-lasting persistent atrial fibrillation: clinical outcome and mechanisms of subsequent arrhythmias. J Cardiovasc Electrophysiol. 2005;16:1138–47.
7. Jais P, Sanders P, Hsu LF, Hocini M, Sacher F, Takahashi Y, et al. Flutter localized to the anterior left atrium after catheter ablation of atrial fibrillation. J Cardiovasc Electrophysiol. 2006;17:279–85.
8. Kobza R, Hindricks G, Tanner H, Schirdewahn P, Dorzewski A, et al. Late recurrent arrhythmias after ablation of atrial fibrillation: incidence, mechanisms and treatment. Heart Rhythm. 2004;1:676–83.

9. Gerstenfeld EP, Callans DJ, Dixit S, Russo AM, Nayak H, Lin D, et al. Mechanisms of organized left atrial tachycardias occurring after pulmonary vein isolation. Circulation. 2004;110:1351–7.
10. Deisenhofer I, Estner H, Zrenner B, Schreieck J, et al. Left atrial tachycardia after circumferential pulmonary vein ablation for atrial fibrillation: incidence, electrophysiological characteristic, and results of radiofrequency ablation. Europace. 2006;8:573–82.
11. Veenhuysen GD, Knecht S, O'Neill Phil D, Wright M, Nault I, Weerasooriya R, et al. Atrial tachycardias encountered during and after catheter ablation for atrial fibrillation: part I: classification, incidence, management. Pacing Clin Electrophysiol. 2009;32: 393–8.
12. Sawhney N, Anousheh R, Chen W, Feld GK. Circumferential pulmonary vein ablation with additional linear ablation results in an increased incidence of left atrial flutter compared with segmental pulmonary vein isolation as an initial approach to ablation of paroxysmal atrial fibrillation. Circa Arrhythmia Electrophysiol. 2010;3:243–8.
13. Chugh A, Oral H, Lemola K, Hall B, Cheung P, et al. Prevalence, mechanisms, and clinical significance of macroreentrant atrial tachycardia during and following left atrial ablation for atrial fibrillation. Heart Rhythm. 2005;2:464–71.
14. Wazni OM, Saliba W, Fahmy T, Lakkireddy D, Thal S, et al. Atrial arrhythmias after surgical maze: findings during catheter ablation. J Am Coll Cardiol. 2006;48:1405–9.
15. Weerasooriya R, Jais P, Wright M, Matsuo KS, et al. Catheter ablation of atrial tachycardia following atrial fibrillation ablation. J Cardiovasc Electrophysiol. 2009;20:833–8.
16. Eitel C, Hindricks G, Dagres N, Sommer P, Piorkowski C. Ensite Velocity cardiac mapping system: a new platform for 3D mapping of cardiac arrhythmias. Expert Rev Med Devices. 2010;7(2):185–92.
17. Ballin SJ, Korthas MA, Weers NJ, Hoffman CJ. Direct visualization of the slow pathway using voltage gradient mapping: a novel approach for successful ablation of atrioventricular nodal reentry tachycardia. Europace. 2011;13(8):1188–94.
18. January CT, Wann LS, Alpert JS, Calkins H, Cigarroa JE, Cleveland JC Jr, Conti JB, Ellinor PT, Ezekowitz MD, Field ME, Murray KT, Sacco RL, Stevenson WG, Tchou PJ, Tracy CM, Yancy CW. AHA/ACC/HRS guideline for the management of patients with atrial fibrillation: executive summary: a report of the American College of Cardiology/American Heart Association Task Force on practice guidelines and the Heart Rhythm Society Circulation. 2014;130(23):2071–104.
19. Coffey JO, d'Avila A, Dukkipati S, Danik SB, Gangireddy SR, et al. Catheter ablation of scar-related atypical atrial flutter. Europace. 2013;15:414–9.
20. Patel AM, d'Avila A, Neuzil P, Kim SJ, Mela T, et al. Atrial tachycardia after ablation of persistent atrial fibrillation: identification of the critical isthmus with a combination of multielectrode activation mapping and targeted entrainment mapping. Circ Arrhythmia Electrophysiol. 2008;1:14–22.
21. Casella M, Perna F, Russo AD, Pelargonio G, et al. Right ventricular substrate mapping using the Ensite Navx system: accuracy of high-density voltage map obtained by automatic point acquisition during geometry reconstruction. Heart Rhythm. 2006:1598–605.
22. Winkle RA, Moskovitz R, Mead RH, Engel G, Kong MH, Fleming W, Patrawala RA. Ablation of atypical atrial flutter using ultra high density-activation sequence mapping. J Interv Card Electrophysiol. 2017;48(2):177–184.
23. Jais P, Matsuo S, Knecht S, Weerasooriya R, Hocini M, et al. A deductive mapping strategy for atrial tachycardia following atrial fibrillation ablation: importance of localized reentry. J Cardiovasc Electrophysiol. 2009;20:480–91.